

Measurement of the thermal conductivity of nanofluids by the multicurrent hot-wire method

José R. Vázquez Peñas, José M. Ortiz de Zárate,^{a)} and Mohamed Khayet^{b)}
Facultad de Física, Departamento de Física Aplicada I, Universidad Complutense, 28040 Madrid, Spain

(Received 29 April 2008; accepted 17 June 2008; published online 27 August 2008)

We present experimental results of the thermal conductivity of several nanofluids prepared by dispersing nanoparticles of SiO₂ and CuO in water and ethylene glycol at various concentrations up to ≈5% in mass fraction. The measurements have been performed by the multicurrent hot-wire technique. Good agreement, within 2%, is found in recommended and published thermal conductivities of the pure fluids. Our experimental technique allows a very accurate determination of the enhancement in the thermal conductivity of the fluids due to the presence of dispersed nanoparticles. Measured enhancements compare well with some of the values published so far in the literature. We have compared our results with simple theoretical models that predict the thermal conductivity of solid suspensions and found that in some cases observed enhancements are several times larger than the predicted ones. © 2008 American Institute of Physics.

[DOI: [10.1063/1.2970086](https://doi.org/10.1063/1.2970086)]

I. INTRODUCTION

During the past decade we have seen an increasing interest in the measurement and modelization of the transport properties of nanofluids, i.e., dispersions of nanoparticles in the bulk of simple fluids. Among the various transport properties, thermal conductivity λ has received the most attention. Pioneering experimental work by Eastman *et al.*^{1,2} reported large thermal conductivity enhancements, $\Delta\lambda$, when a little amount of nanoparticles is added to a liquid. Subsequent experimental studies³⁻⁸ confirmed the large $\Delta\lambda$ values and established that standard theoretical models for the thermal conductivity of solid suspensions, such as the classical Maxwell⁹ model, could not explain the large enhancements observed. This recent experimental work extended preceding results referred to suspensions of microparticles, as summarized elsewhere.¹⁰

Theoretical work, trying to explain the anomalous thermal conductivity enhancement in nanofluids, followed the experiments.¹¹ Several physical mechanisms that may enhance the λ of nanofluids were discussed by Keblinski *et al.*,¹² among them the Brownian motion of the particles and aggregation or percolation. Some authors¹³ developed a controversial model that tried to incorporate both the size of the particles (surface area to volume ratio) and their Brownian motion. The idea of incorporating surface area to volume ratio in the theory was further developed recently by Vadasz.¹⁴ The Brownian motion contribution to $\Delta\lambda$ was also further developed recently¹⁵ but only at a phenomenological level. Aggregation (cluster formation) and adsorbed layers were considered by Xuan *et al.*¹⁶ More recently, it was demonstrated at a very fundamental level¹⁷ that the formation of percolating structures breaks the Maxwell limit for the thermal conductivity of solid suspensions in liquids.

Before definitively settling the theoretical problem many experimental issues need to be solved. Although most researches in the field have consistently reported enhancements beyond the Maxwell model, there exists a large scattering in the $\Delta\lambda$ values reported by different laboratories for the same nanofluid.¹⁸ In some cases, differences larger than the enhancement itself can be found in the literature [see, for instance, the discussion of the CuO/ethylene glycol (EG) system later in Sec. IV]. Of course, these disagreements may be caused by the different particle sizes and/or polydispersivities, as discussed by Kumar *et al.*¹³ However, different sample preparations and stabilization methods seem also to play a role.¹⁹

Finally, as it has been discussed extensively by several authors,^{1,11,18} the existence of a large enhancement in the thermal conductivity of nanofluids is not just a fancy theoretical issue since it may have important technological consequences. Particularly, the addition of nanoparticles in coolant fluids could improve their heat transfer properties, and it paved the way for the design of tailored refrigerants.

We have organized the material to be presented as follows. First, in Sec. II, we describe the preparation of our nanofluid samples and discuss the experimental method used to measure their thermal conductivity. In Sec. III we present the experimental results obtained, first for pure liquids, water, and EG, and then for the seven different nanofluids employed. Finally, in Sec. IV, we discuss our results, comparing them with other experimental values and with various theoretical models proposed for the prediction of the thermal conductivity of nanofluids.

II. PREPARATION OF THE SAMPLES AND EXPERIMENTAL METHOD

It is believed that the strong scattering in the experimental data of the thermal conductivity of nanofluids is related to the different sample preparations. For this reason we shall

^{a)}Electronic mail: jmortizz@fis.ucm.es.

^{b)}Author to whom correspondence should be addressed. Electronic mail: khayetm@fis.ucm.es.

describe in detail how our samples were prepared before briefly discussing the experimental technique used to measure their thermal conductivity.

A. Preparation of the samples

The liquids employed in this research to prepare the nanofluids were water and EG. Water was prepared in our laboratory by double distillation. Before using it for the experiments it was verified that the electrical resistivity was larger than 15 M Ω cm. The liquid EG was supplied by Panreac Química S.A. (Barcelona, Spain) with 99.5% nominal purity and used without further purification.

In this investigation we have employed commercial nanopowders supplied by Sigma-Aldrich. Silica (SiO₂) nanopowder is described by the manufacturer (Catalog No. S5505-100G) as having an average particle size of 14 nm and surface area of 200 \pm 25 m² g. Copper oxide (CuO) nanopowder is described by the manufacturer (Catalog No. 544868-25G) as having an average particle size of 33 nm and surface area of 29 m² g.

Nanofluids were prepared by weighing in a balance having a precision of \pm 0.05 g. Seven nanofluids were prepared: three based on water (W1–W3) and four based on EG (EG1–EG4). W1 was prepared by dispersing 4.8% (weight fraction, w/w) of SiO₂ nanoparticles, W2 was prepared by dispersing 2.4% (w/w) of CuO nanoparticles, and W3 was prepared by dispersing 4.8% (w/w) of CuO nanoparticles. EG1 was prepared by dispersing 2.3% (w/w) of SiO₂ nanoparticles, EG2 was prepared by dispersing 4.8% (w/w) of SiO₂ nanoparticles, EG3 was prepared by dispersing 2.2% (w/w) of CuO nanoparticles, and EG4 was prepared by dispersing 4.6% (w/w) of CuO nanoparticles. Estimations of the volume fraction of particles in these nanofluids are discussed in Sec. III B.

Dispersions were performed only by physical means, without using any chemical additive (surfactant, pH buffer, or any other kind). Mixtures were first strongly stirred mechanically and later subjected to ultrasonics (150 W power) for at least $\frac{1}{2}$ h to break up any residual agglomerations. After this procedure very homogeneous dispersions were produced. It is well known that the most difficult issue when working with nanofluids is sample stability.²⁰ Nanoparticles tend to sediment at the bottom of the samples, causing the physical properties of the bulk nanofluid to change with time. In our case, the measurement of the thermal conductivity of the nanofluid requires temperature cycling and many individual measurements (see Sec. II B) that require at least 1 week.

In our research, special care has been taken to check sample stability. After finalizing the measurements we checked the samples and found no visible sedimentation. Furthermore, in some cases we repeated the temperature cycling of the measurements (without further stirring of the samples), looking for differences in the measured λ that might indicate lack of stability in the sample. We found no differences larger than the accuracy of the measurement. The concentration of nanoparticles in our nanofluids may seem

smaller than in other investigations because we discharged higher concentrations for which we could not get reproducibility for a period of 2 weeks.

However, after months of storage in the laboratory, most samples investigated showed sedimentation. In general, nanofluids based on EG presented less particle deposition than those based on water. This behavior is expected due to the large differences in viscosity. A particularly interesting case is the dispersion of silica nanoparticles in EG, which showed extraordinary stability, even after 1 year of storage.

In spite of the comments in the previous paragraph, we stress that the results to be presented here were all obtained in the first weeks after sample preparation and were checked for reproducibility. In this study only λ values are reported for nanofluids showing reproducibility and sample homogeneity during the measurement period.

B. Experimental method

Our values for the thermal conductivity of the nanofluids were obtained by the transient multicurrent hot-wire technique. Nowadays this technique is accepted as the most precise and reliable method to measure the thermal conductivity of fluids over a wide range of temperatures and pressures. The measurements can deliver absolute values (do not require comparison with any standard), and only knowledge of the hot-wire geometry, the applied intensity, and the electrical resistance of the wire is required. For the best experiments, the accuracy of the results is estimated to be \pm 0.5%.^{21,22}

The experimental setup and method employed in this investigation is essentially similar to the one recently used in our laboratory for the absolute measurement of the thermal conductivity of several glycols.²³ Consequently only a brief description will be given here, and we refer the reader to previous publications²³ for further details.

The core of our experimental setup is a platinum wire of 50 μ m diameter and 21.47 \pm 0.01 cm length. The wire is supported by a chemically resistant frame to keep it straight, and two Teflon isolated leads were connected to each of the wire ends. The four connectors were electrically insulated by coating with chemically resistant epoxy. Furthermore, to avoid electrical contact between the platinum wire and the liquids, the whole set (including the wire itself and the frame supporting it) was covered with a Teflon-based industrial coating. The thickness of this coating is less than 1 μ m.

A Keithley 2400 source meter, which can act simultaneously as current source and voltage meter, was employed. This instrument is interfaced to a personal computer and a software code was developed to retrieve the measurement points, fit the data, and calculate the thermal conductivity (see below). For each measurement, various current values, from 260 to 360 mA, were applied. The electrical current is injected by two of the leads connected to the wire ends, while voltage measurements are acquired simultaneously using the other two leads. The supported wire is placed vertically inside a double wall glass cell, which is connected to a thermostatic bath to control the temperature at which the experiments are performed within \pm 0.05 K. The liquid un-

der testing was loaded in the inner volume of the glass cell. The whole assembly (glass cell containing the wire) is then placed inside a controlled atmosphere chamber. A platinum resistance thermometer placed inside the cell is used to measure the temperature of the liquid under testing. This thermometer is also interfaced to the personal computer controlling the experiment and the same computer code manages simultaneously the thermometer and the electrical source meter.

When an electric current I is circulated through the wire, because of Joule heating, the wire temperature increases. While the liquid is quiescent, the rate of wire heating depends only on the thermal conductivity and the thermal diffusivity of the liquid surrounding the wire as discussed, for instance, by Carslaw and Jaeger.²⁴ As a consequence of the heating, the electrical resistance of the wire, R , increases as does the voltage drop between the wire ends, V . For an infinitely cylindrical straight wire, the voltage difference between two points, separated by a distance L , can be approximated by²⁵

$$V(t) \approx IR_0 \left\{ 1 + \alpha \frac{I^2 R_0}{4\pi\lambda L} \left[\ln\left(\frac{t}{\beta}\right) - \gamma \right] \right\}, \quad (1)$$

where R_0 is the electrical resistance of the wire at $t=0$, γ is Euler's constant ($\gamma=0.5770$), α is the temperature resistance coefficient of the material of the wire, λ is the thermal conductivity of the liquid surrounding the wire, and L is the wire length. Parameter β (units of time) is expressed as

$$\beta = \frac{r_0^2}{4a}, \quad (2)$$

with a being the thermal diffusivity of the liquid surrounding the wire and r_0 the wire radius. Equation (1) is valid as an asymptotic expansion for a long time $t \gg \beta$. In deducing Eq. (1) self-heating effects in the wire are neglected and the liquid surrounding the wire is assumed to be in a quiescent state (no convection). Recently²⁶ improvements have been proposed in the analysis of heating curves based on a finite element modeling of the heat transfer problem instead of using asymptotic expansions such as Eq. (1). Implementation of these refinements may increase the accuracy of our method in future studies.

In our experiments, a typical heating run lasts for a couple of seconds during which 350 voltage measurements are acquired. Moreover, before each heating run, a resistance measurement is performed using the four-wire configuration of the Keithley 2400, which compensates for the electrical resistance of the connecting leads. Furthermore, a temperature reading is also recorded. The thermal conductivity is then obtained by fitting, as required by Eq. (1), the data pairs $[\Delta V_i, \ln(t_i)]$ acquired in a heating run into a straight line, from which slope b is obtained. Since Eq. (1) is an asymptotic expansion for large t , only the points acquired after ≈ 213 ms are actually used in the fitting procedure. From slope b the thermal conductivity is obtained as

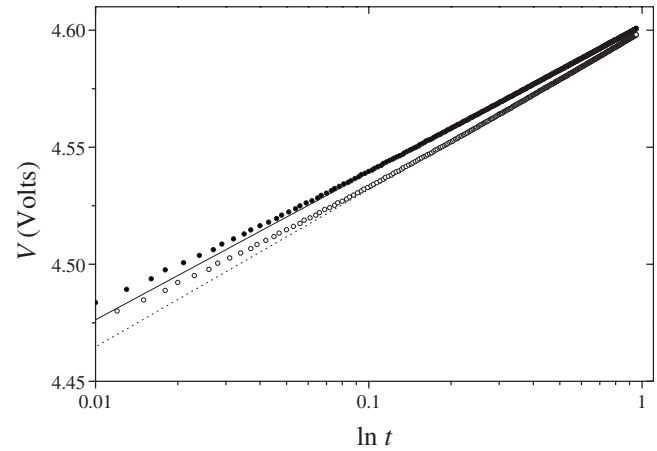


FIG. 1. Typical individual heating curves: voltage drop in the wire, V , as a function of time t . Open symbols are for pure EG and filled symbols are for the nanofluid prepared by dispersing silica nanoparticles in glycol at 4.8% (w/w). In both cases the initial temperature was 60 °C and $I=320$ mA. Straight lines represent fittings to Eq. (1) of the points measured after ≈ 213 ms.

$$\lambda = \frac{mI^2 R_0}{4\pi L b}, \quad (3)$$

where I is the intensity value programmed in the source meter is used and R_0 is the value measured just before each heating run is substituted. The quantity $m=\alpha R_0$ represents the slope of the R - T curve at the initial temperature of the heating run.

As an example of the individual heating runs, we show in Fig. 1 two typical heating curves, where the voltage drop in the platinum wire is displayed as a function of time in a semilogarithmic scale. Data are shown for pure EG and for dispersion of silica nanoparticles in glycol at 4.8% (w/w). In both cases the initial temperature was 60 °C and the heating current was $I=320$ mA. The data displayed in Fig. 1 show that the experimental results are asymptotically very well represented by Eq. (1) and that no convection is present in the liquid.

For a given temperature, we have performed thermal conductivity measurements using different values of the current I . This procedure is referred to as multicurrent hot wire, and it gives more reliable values of λ since there is a very slight correlation between the measured λ values and the intensity I employed to obtain it, within the quoted accuracy for λ . This issue has been discussed in more detail elsewhere.²³ For this work we have performed quite large statistics, and the values to be presented in Sec. III for each temperature were obtained by averaging over a couple hundred individual λ measurements taken at six different values of the heating current. This large and redundant number of individual measurements corresponds typically to ≈ 20 h of continuous operation of our apparatus.

Consequently, the thermal conductivity of the fluid under test is obtained, via Eq. (3), from slopes b of fittings such as the ones shown in Fig. 1 plus the knowledge of the current I at which the heating was conducted and a direct measurement of the electrical resistance R_0 of the wire before each heating run. The slope $m=\alpha R_0$ of the resistance-temperature curve and the length L of the wire are also required.

For the temperature resistance coefficient α , tabulated values for platinum could be initially used. However, more accurate λ results are obtained if the “experimental” slope m is used.²³ As explained before, with our experimental device we are acquiring simultaneous temperature and electrical resistance pairs just before each heating run. We can, thus, fit these pairs into a linear trend and obtain an experimental value of m for the particular wire one uses. Furthermore, this procedure allows for an independent check of the stability and the accuracy of the experiment. Indeed, we have found excellent reproducibility among the electrical resistance of the wire versus temperature curves obtained with the various fluids and nanofluids used in this investigation, differences in electrical resistance of the wire being always less than 1%. This demonstrates that current leak through the liquid is not important in spite of the different electrical conductivities of the fluids.

The R - T experimental data fit extremely well into a linear trend at the temperature range used in this investigation: 20–80 °C. When extrapolated to 0 °C our data give an average temperature coefficient of resistance $\alpha = 0.00390 \pm 0.0005$, in agreement with tabulated values for platinum. The length L of the wire has been measured with a cathetometer with an accuracy of ± 0.01 cm.

III. EXPERIMENTAL RESULTS

The accuracy of the λ values obtained by the procedure described in Sec. II B is mainly determined by the validity of Eq. (3), thus, by limitations of the theory. Effects such as finite length of the wire,²⁵ leaking by radiation,²⁷ compression work,²⁸ and timing of voltage measurements are not accounted for in Eqs. (1)–(3). All these factors contribute as systematic errors (or bias) and limit the accuracy of the absolute measurements to a few percent that, for our particular setups, has been estimated as 2.5%–3%.²³

An alternative approach that can give more accurate λ values is to perform relative measurements, i.e., to rewrite Eq. (3) as

$$\lambda = A \frac{I^3 R_0}{b}, \quad (4)$$

where A is a “calibration” constant that it is assumed not to depend on the fluid under test. A calibration fluid whose thermal conductivity is known can be used to infer a value for A . If measurements are performed at various temperatures, a better estimation of the calibration constant can be obtained by simultaneous comparison with a set of tabulated $\lambda(T)$. Once A is determined, this value is used to evaluate the thermal conductivity of a test fluid. Initially, the calibration parameter A includes the length of the wire and the slope of the R - T straight line, but it also represents all unknown sources of systematic errors. We estimate that this calibration method improves the accuracy of our λ values, reducing the contribution of systematic errors from 3% to around 0.5%.

Notice that this calibration procedure is especially well suited for the study of the thermal conductivity of nanofluids.

TABLE I. Experimental values of the thermal conductivity of water and EG at various temperatures. Only statistical errors are reported here.

EG		Water	
T (°C)	λ (W/mK)	T (°C)	λ (W/mK)
19.9	0.2473 ± 0.0015	20.4	0.6070 ± 0.0025
39.3	0.2526 ± 0.0020	40.2	0.6382 ± 0.0014
58.9	0.2572 ± 0.0018	60.1	0.6584 ± 0.0020
78.5	0.2614 ± 0.0021		

For nanofluids one is usually specifically interested in reporting the so-called thermal conductivity enhancement, $\Delta\lambda$, defined as¹⁸

$$\Delta\lambda(\%) = \frac{\lambda_{\text{nanofluid}} - \lambda_{\text{liquid}}}{\lambda_{\text{liquid}}} 100. \quad (5)$$

From Eq. (4), it is obvious that if one uses the pure liquid on which the nanofluid is based as the calibration fluid, the experimental enhancement in the thermal conductivity is insensitive to the calibration constant A ; thus, very accurate values for $\Delta\lambda$ can be reported.

Having in mind the previous discussion, we split the presentation of the experimental results into two blocks. First, in Sec. III A we present the results obtained for pure fluids. In this case we present absolute measurements obtained directly from the measured values of $m = \alpha R_0$ and L . These λ values have a systematic error of about 3% as explained previously. Later, in Sec. III B we present the experimental results obtained for the nanofluids. In this case we use the calibration method, employing as calibrating fluid the liquid on which the nanofluid is based. Only experimental enhancements $\Delta\lambda$ will be reported for the nanofluids. The contribution of systematic errors to the data reported in Sec. III B is reduced below 0.5%.

A. Pure fluids

The pure fluids used in this investigation were water and EG. Thermal conductivity values were obtained by an absolute method, as specified by Eq. (3). Thermal conductivities of EG were measured at four different values of the temperature in the bath, namely, 20, 40, 60, and 80 °C. Measurements at 80 °C were not performed for water because the fluid was close to its boiling point and measurements were less reliable. It was impossible to avoid the buildup of bubbles in the bulk of the liquid.

The values obtained for the thermal conductivity of the pure fluids are reported in Table I. The temperatures in Table I correspond to the average of the temperature measured inside the hot-wire cell and differ slightly from the temperature programmed in the bath. As already mentioned, during each measurement the temperature inside the cell was stable within ± 0.05 K. The error reported in Table I in the thermal conductivity data is the statistical standard deviation of the individual measurements (reproducibility), typically 150 data points at various current values for each temperature. As extensively discussed above, a 3% systematic error has to be added to the thermal conductivity data reported in Table I.

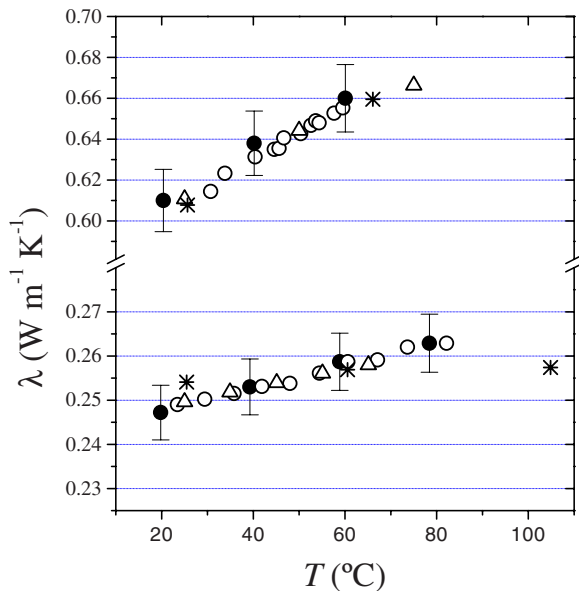


FIG. 2. (Color online) Comparison of the thermal conductivity values obtained in this research (filled circles) with several literature values. For water (top panel) triangles are from the ASTM-D2717 standard, empty circles are from Assael *et al.* (Ref. 30), and asterisks are from Bohne *et al.* (Ref. 31). For EG (bottom panel) triangles are from Khayet and Ortiz de Zárate (Ref. 23), empty circles are from Assael *et al.* (Ref. 30), and asterisks are from DiGiulio and Teja (Ref. 32).

The data reported in Table I are displayed graphically in Fig. 2, together with some selected literature values for comparison. The error bars in Fig. 2 have been calculated by adding a 3% systematic error to the standard deviations reported in Table I. An inspection of the data displayed in Fig. 2 shows that our present results agree with literature values within the experimental uncertainty.

From plots such as the ones displayed in Fig. 2, calibration constants A are deduced, as explained above, for later use in the determination of the $\Delta\lambda$ of the nanofluids. For instance, in the case of water, we found that tabulated data are better represented by an A constant that is about 2% lower than the value of $m/4\pi L$. This difference is within the quoted accuracy of our measurements.

B. Nanofluids

The thermal conductivity enhancement of seven different nanofluids has been measured in the present investigation. The nanofluids were prepared by dispersing SiO_2 and CuO nanopowder in water and EG. Three nanofluids were

based on water (W1–W3), and four nanofluids were based on EG (E1–E4). The nanofluid preparation and the weight fraction concentration of the various samples were described in Sec. II A.

The volume fraction of particles, ϕ , has been estimated from the densities of the liquids and of the bulk solid oxides at 20 °C. These densities were obtained from standard thermodynamic tables. We note that there is a huge difference between the densities of the bulk solids and the corresponding nanopowders. This is most likely caused by the strong electrostatic repulsion among the particles. Once the nanofluids are prepared, and if the particles are indeed well dispersed in the liquid, we believe that a correct estimation of ϕ is obtained from the density of the solids. Estimated values for the volume fraction of particles, ϕ , are displayed in the second row of Table II for nanofluids based on water and in the second row of Table III for nanofluids based on EG.

As discussed in Sec. III, thermal conductivity measurements of the nanofluids have been performed by the calibration method using the corresponding pure liquid as calibration fluid. The thermal conductivity values are thus based on Eq. (4), and only experimental enhancements $\Delta\lambda$ are reported here. In Tables II and III, experimental enhancements obtained in this investigation are displayed for nanofluids based on water and on EG, respectively. Small temperature differences between the actual average temperatures used for the pure liquid and the nanofluids were unavoidable. For the evaluation of the experimental $\Delta\lambda$ we have used as reference for each nanofluid at each temperature the pure liquid data obtained at the same bath temperature.

We do not report errors in the data displayed in Tables II and III. The standard deviation corresponding to the large (≈ 150) series of individual data measured for each nanofluid and each temperature was in all cases less than 0.1%, similar to the statistical deviation of the λ reported for pure liquids in Table I. Furthermore, values of the thermal conductivity enhancement $\Delta\lambda$ have been obtained by the calibration method, so we estimate that they are free from systematic errors up to 0.5%. As a conclusion, precision of the values reported in Tables II and III is $\pm 0.01\%$ for all $\Delta\lambda$ values displayed. For this reason, and for the sake of clarity, we preferred not to explicitly show experimental errors in Tables II and III.

IV. DISCUSSION

The first observation we can infer from the data displayed in Tables II and III is that the enhancement in the

TABLE II. Estimated values of the volume fraction of particles, ϕ , and experimental values of the enhancement in thermal conductivity of nanofluids based on water. Thermal conductivity enhancement is reported in percentage. See main text for comments on uncertainties.

W1: SiO_2 (14 nm) 4.8% (w/w), $\phi \approx 2.2\%$		W2: CuO (33 nm) 2.4% (w/w), $\phi \approx 0.4\%$		W3: CuO (33 nm) 4.9% (w/w), $\phi \approx 0.8\%$	
T (°C)	$\Delta\lambda$	T (°C)	$\Delta\lambda$	T (°C)	$\Delta\lambda$
20.4	3.04	20.3	0.44	20.3	1.59
44.8	3.49	40.1	1.11	40.0	2.92
60.5	1.41	60.3	2.95	60.1	4.65

TABLE III. Estimated values of the volume fraction of particles, ϕ , and experimental values of the enhancement in thermal conductivity of nanofluids based on EG. Thermal conductivity enhancement is reported in percentage. See main text for comments on uncertainties.

EG1: SiO ₂ (14 nm) 2.3% (w/w), $\phi \approx 1.2\%$		EG2: SiO ₂ (14 nm) 4.8% (w/w), $\phi \approx 2.5\%$		EG3: CuO (33 nm) 2.2% (w/w), $\phi \approx 0.4\%$		EG4: CuO (33 nm) 4.6% (w/w), $\phi \approx 0.8\%$	
T (°C)	$\Delta\lambda$	T (°C)	$\Delta\lambda$	T (°C)	$\Delta\lambda$	T (°C)	$\Delta\lambda$
19.9	0.79	20.6	3.61	20.3	2.51	20.6	5.85
39.7	0.58	40.5	4.13	39.7	3.06	42.3	6.01
59.0	1.53	60.5	4.42	58.4	4.22	60.1	6.27
79.0	1.47	80.2	4.42	80.1	3.20	79.8	5.35

thermal conductivity of all the nanofluids investigated at all temperatures is always positive. Hence, the addition of nanopowders systematically increases the thermal conductivity of the nanofluid, as compared with the pure liquid. This fact is true for the two liquids and the two nanopowders at all the concentrations and temperatures investigated.

For a given nanofluid, the experimental enhancement $\Delta\lambda$ reported in Tables II and III seems to be almost independent of the temperature. For the nanofluids obtained by dispersing copper oxide nanoparticles in water, it seems that there is a systematic increase in $\Delta\lambda$ with the temperature, but this trend is not confirmed in the other nanofluids investigated. Furthermore, the statistical significance of this trend is very marginal since the apparent increase in the CuO/W, $\Delta\lambda$, is almost within the experimental uncertainty of the measurements. We note that some authors^{3,10} reported $\Delta\lambda$ that increase with the temperature, as sketched here by the CuO/W data. However, and to be fair, from our present data and at the temperature range studied, we have to conclude that $\Delta\lambda$ is independent of the temperature, at least within the accuracy of our measurements. As a consequence, we have evaluated average enhancements for each nanofluid, and from now on we continue our discussion in terms of these average enhancements. In the second column of Table IV we display these average experimental enhancements for the different nanofluids investigated.

In Fig. 3 we show graphically the experimental values

TABLE IV. Comparison between the experimental enhancements $\Delta\lambda_{\text{expt}}$ and the predictions based on the two-layer model of Eq. (6), $\Delta\lambda_{2\text{lay}}$ and the Maxwell–Hamilton and Crosser model of Eq. (7), $\Delta\lambda_{\text{max}}$. The different nanofluids are as indicated.

Mixture	$\Delta\lambda_{\text{expt}}$ (%)	$\Delta\lambda_{2\text{lay}}$ (%)	$\Delta\lambda_{\text{max}}$ (%)
SiO ₂ /W			
$\phi=2.2\%$	2.65	1.19	1.84
CuO/W			
$\phi=0.4\%$	1.50	0.39	1.08
$\phi=0.8\%$	3.06	0.78	2.18
SiO ₂ /EG			
$\phi=1.2\%$	1.09	0.98	2.13
$\phi=2.5\%$	4.14	2.07	4.47
CuO/EG			
$\phi=0.4\%$	3.25	0.40	1.15
$\phi=0.8\%$	5.87	0.79	2.32

for $\Delta\lambda$, averaged over the temperature as reported in the second column of Table IV, versus the volume fraction ϕ of nanoparticles. Our present experimental results are represented by symbols, as indicated in the figure, while several literature values are also plotted for comparison. In addition three lines displayed in Fig. 3 represent the trend of our data. The line with the higher slope represents the trend of the CuO/EG nanofluid, the line with intermediate slope represents the trend for the CuO/water nanofluid, and the line with lower slope represents the trend of the silica nanofluids. In the latter case we are not able to distinguish between the results of water and EG, so we have plotted a single line representing both liquids. Literature values plotted in Fig. 3 are as follows: asterisks (*) represent data from Lee *et al.*⁴ for CuO/water nanofluids (24 nm particle size), crosses (+) represent a combination of data from Lee *et al.*⁴ and from Kwak and Kim⁵ for CuO/EG nanofluids (24 and 12 nm particle sizes, respectively), and a single star (★) represents a measure by Eastman *et al.*² also for a CuO/EG nanofluid (36 nm particle size). For silica nanofluids we have not found published values so far; thus we added to Fig. 3 Al₂O₃ measurements (×) from Lee *et al.*⁴ for comparison (38 nm par-

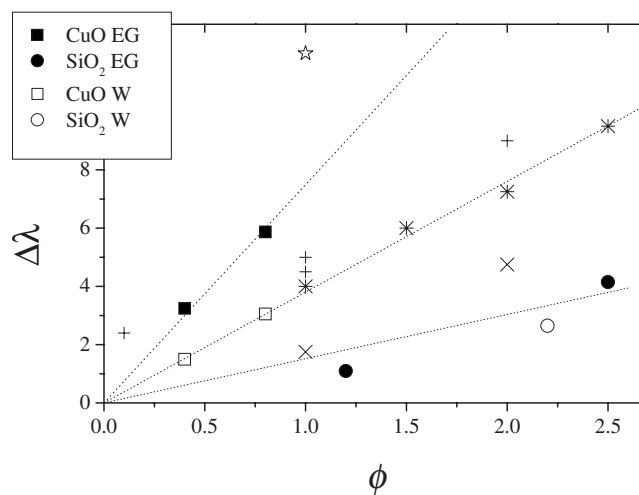


FIG. 3. Thermal conductivity enhancement (%) as a function of the volume fraction ϕ of nanoparticles (%). Squares and circles are data obtained in this research (as indicated). Other symbols represent several literature values: Lee *et al.* (Ref. 4) (*) for CuO/Water nanofluids, Lee *et al.* (Ref. 4) and Kwak and Kim (Ref. 5) (+) for CuO/EG nanofluids, and Eastman *et al.* (Ref. 2) (★) also for a CuO/EG nanofluid. For comparison with our silica data we add Al₂O₃ measurements (×) from Lee *et al.* (Ref. 4). The straight lines are simple guide to the eyes representing the trend of our data.

ticle size). There are much more experimental data published, as reviewed elsewhere,¹⁸ but we decided not to add more literature data points to Fig. 3 to keep it readily understandable.

A simple examination of Fig. 3 allow us to reach several conclusions. (i) We obtained larger enhancements for nanofluids with CuO than for nanofluids with silica. This finding is consistent with published data if we compare silica with alumina, which is probably the closest (in $\Delta\lambda$) nanopowder studied so far in the literature. This difference can be explained in terms of simple thermal conductivity models (see below). (ii) Our present experimental results compare well with some published data. For instance, we find excellent agreement between the trend of our current data for CuO/water and published values by Lee *et al.*⁴ In contrast, for the case of CuO/EG nanofluids the agreement is worse. We get for this mixture results that are intermediate between those from Eastman *et al.*² and the combination of those from Lee *et al.*⁴ and Kwak and Kim.⁵ This poor agreement between different experiments is typical in nanofluid studies as mentioned in Sec. I, demonstrating that further experimental work is required. To finalize, we note that our results for silica nanofluids are consistent with published data for alumina.

It is worth mentioning, however, that our present results for $\Delta\lambda$ are significantly lower than some other published data. For instance, the enhancement we measure for CuO/water nanofluids is about one-half of the one reported by Li and Peterson¹⁰ for 19 nm CuO nanoparticles. Similar differences exist with values reported by Das *et al.*³ In these two cases, while not completely clear, it seems like such a big difference is related to different methods in the estimation of ϕ .

One interesting issue concerning the thermal conductivity of nanofluids is if the observed enhancements can be explained in terms of existing theoretical models. Recently, Wang and Mujumdar¹⁸ extensively reviewed different theories that have been proposed to explain the thermal conductivity of suspensions of particles in fluids, beginning with the adaptation by Hamilton and Crosser²⁹ of the classical Maxwell⁹ model, initially developed to predict the dielectric properties of a suspension of microspheres. In addition to all the specific models described by Wang and Mujumdar,¹⁸ we think it is quite insightful to consider also the naive idea of modeling the nanofluid as a series of two layers, one of particles and the other of pure fluid. In this case, a very simple exercise shows that the “effective” thermal conductivity of the composite layer can be expressed as

$$\frac{1}{\lambda_{\text{eff}}} = \frac{\phi}{\lambda_p} + \frac{1-\phi}{\lambda_f}, \quad (6)$$

where λ_p is the thermal conductivity of the particles and λ_f the thermal conductivity of the pure fluid.

We do not plan to compare here our experimental data with all the theoretical models proposed so far and discussed elsewhere.¹⁸ Furthermore, as also reviewed in Ref. 18 for small concentrations in volume fraction (as the data we present here), there is little difference between the classical Maxwell model and the other more sophisticated theories.

Consequently, in addition to the two-layer model of Eq. (6), we shall compare our current experimental data only with the classical Maxwell–Hamilton and Crosser model.^{9,29} This model considers a suspension of spherical solid particles in a liquid and predicts theoretically an effective thermal conductivity that can be expressed as^{11,18}

$$\frac{1}{\lambda_{\text{eff}}} = \frac{1}{\lambda_f} - \frac{\phi}{\lambda_f \lambda_p} \frac{3(\lambda_p - \lambda_f)}{2\lambda_p + 2(\lambda_p - \lambda_f)\phi}. \quad (7)$$

In Table IV we show the experimental values of the thermal conductivity enhancement $\Delta\lambda_{\text{expt}}$ (obtained by averaging over temperature the data displayed in Tables II and III), together with the predictions based on the two-layer model of Eq. (6) and the Maxwell model of Eq. (7), for the different nanofluids studied in the present investigation. To evaluate the model predictions we took the pure fluid thermal conductivity from the data at 20 °C reported in Table I. For the thermal conductivity of the particles, we used tabulated values for the bulk solids: $\lambda_{\text{CuO}} = 17 \text{ W m}^{-1} \text{ K}^{-1}$ and $\lambda_{\text{SiO}_2} = 1.3 \text{ W m}^{-1} \text{ K}^{-1}$ (noncrystalline).

An inspection of the values reported in Table IV shows that theoretical enhancements calculated by using the two-layer model of Eq. (6) are in all cases several times smaller than the experimental enhancements. Regarding the estimations based on the Maxwell model of Eq. (7), we observe that for the nanofluids containing silica particles it gives quite a reasonable estimation. However, for the nanofluids containing copper oxide particles, estimations based on the Maxwell model also fail. As anticipated, it seems that the larger enhancement presented by CuO nanofluids, as compared with silica, can be explained by the λ difference between the corresponding solids.

We conclude our investigation by noting that the enhancement in the thermal conductivity of nanofluids is properly regarded as anomalous. As discussed by other investigators,^{11,18} we also conclude that there is no reliable theory to predict the anomalous thermal conductivity of nanofluids yet available. Whether the differences are due to the Brownian motion of the particles, to surface effects, to cluster formation, or to any other cause is still an open question worthy of further investigation¹¹ both theoretically and experimentally. We look forward to seeing more developments in this extremely interesting topic in the coming future.

ACKNOWLEDGMENTS

We have greatly appreciated stimulating discussions with Manuel M. Piñeiro from the University of Vigo (Spain). We are also indebted to the Spanish Ministerio de Educación y Ciencia (Contract No. FIS2006-05323) for supporting this research.

¹J. A. Eastman, S. U. S. Choi, S. Li, W. Yu, and L. J. Thompson, *Appl. Phys. Lett.* **78**, 718 (2001).

²J. A. Eastman, S. U. S. Choi, S. Li, L. J. Thompson, and S. Lee, in *Materials Research Society Symposium Proceedings No. 457* (Materials Research Society, Pittsburgh, PA, 1997), pp. 3–11.

³S. K. Das, N. Putra, P. Thiesen, and W. Roetzel, *J. Heat Transfer* **125**, 567 (2003).

⁴S. Lee, S. U. S. Choi, S. Li, and J. A. Eastman, *J. Heat Transfer* **121**, 280

- (1999).
- ⁵K. Kwak and C. Kim, *Korea-Aust. Rheol. J.* **17**, 35 (2005).
- ⁶H. E. Patel, S. K. Das, T. Sundararajan, A. S. Nair, B. George, and T. Pradeep, *Appl. Phys. Lett.* **83**, 2931 (2003).
- ⁷T.-K. Hong, H.-S. Yang, and C. J. Choi, *J. Appl. Phys.* **97**, 064311 (2005).
- ⁸Y. Xuan and Q. Li, *Int. J. Heat Fluid Flow* **21**, 58 (2000).
- ⁹J. C. Maxwell, *A Treatise on Electricity and Magnetism*, 2nd ed. (Clarendon, Oxford, 1881).
- ¹⁰C. H. Li and G. P. Peterson, *J. Appl. Phys.* **99**, 084314 (2006).
- ¹¹K. S. Gandhi, *Curr. Sci.* **6**, 717 (2007).
- ¹²P. Keblinski, S. R. Phillpot, S. U. S. Choi, and J. A. Eastman, *Int. J. Heat Mass Transfer* **45**, 855 (2002).
- ¹³D. H. Kumar, H. E. Patel, V. R. R. Kumar, T. Sundararajan, T. Pradeep, and S. K. Das, *Phys. Rev. Lett.* **93**, 144301 (2004).
- ¹⁴P. Vadasz, *Trans. ASME, Ser. C: J. Heat Transfer* **128**, 465 (2006).
- ¹⁵S. P. Jang and S. U. S. Choi, *Appl. Phys. Lett.* **84**, 4316 (2004).
- ¹⁶Y. Xuan, Q. Li, and W. Hu, *AIChE J.* **49**, 1038 (2003).
- ¹⁷J. Eapen, J. Li, and S. Yip, *Phys. Rev. E* **76**, 062501 (2007).
- ¹⁸X.-Q. Wang and A. S. Mujumdar, *Int. J. Therm. Sci.* **46**, 1 (2007).
- ¹⁹M. M. Piñero, personal communication (October 9, 2007).
- ²⁰Y. Hwang, J. K. Lee, C. H. Lee, Y. M. Jung, S. I. Cheong, C. G. Lee, B. Ku, and S. P. Jang, *Thermochim. Acta* **455**, 70 (2007).
- ²¹Y. Nagasaka and A. Nagashima, *Rev. Sci. Instrum.* **52**, 229 (1981).
- ²²M. J. Assael, E. Charitidou, C. Nieto de Castro, and W. Wakeham, *Int. J. Thermophys.* **8**, 663 (1987).
- ²³M. Khayet and J. M. Ortiz de Zárate, *Int. J. Thermophys.* **26**, 637 (2005).
- ²⁴H. S. Carslaw and J. C. Jaeger, *Conduction of Heat in Solids* (Oxford University Press, Oxford, 1959).
- ²⁵J. Kestin and W. A. Wakeham, *Physica A* **92**, 102 (1978).
- ²⁶M. J. Assael, K. D. Antoniadis, K. E. Kakosimos, and I. N. Metaxa, *Int. J. Thermophys.* **29**, 445 (2008).
- ²⁷C. A. Nieto de Castro, R. Perkins, and H. M. Roder, *Int. J. Thermophys.* **12**, 985 (1991).
- ²⁸M. J. Assael, L. Karagiannidis, S. M. Richardson, and W. A. Wakeham, *Int. J. Thermophys.* **13**, 223 (1992).
- ²⁹R. L. Hamilton and O. K. Crosser, *Ind. Eng. Chem. Fundam.* **1**, 187 (1962).
- ³⁰M. J. Assael, E. Charitidou, S. Augustinianus, and W. A. Wakeham, *Int. J. Thermophys.* **10**, 1127 (1989).
- ³¹D. Bohne, S. Fischer, and E. Obermeier, *Ber. Bunsenges. Phys. Chem.* **88**, 739 (1984).
- ³²R. DiGiulio and A. S. Teja, *J. Chem. Eng. Data* **35**, 117 (1990).